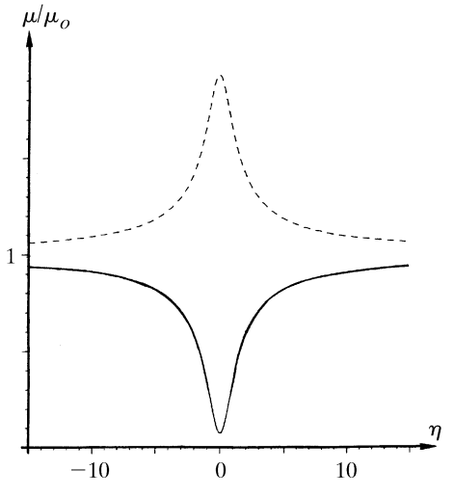

Fig. 5.1.6.1. Variation of the effective absorption with the deviation parameter in the transmission case for the 400 reflection of GaAs using Cu $K\alpha$ radiation. Solid curve: branch 1; broken curve: branch 2.

nodes of the electric field lie on the planes corresponding to the maxima of the *hkl* component of the electron density, the wavefields are absorbed anomalously less than when there is no diffraction. Just the opposite occurs for branch 2 wavefields, whose anti-nodes lie on the maxima of the electron density and which are absorbed more than normal.

The effective absorption coefficient μ is related to the imaginary part of the wavevectors through (5.1.2.19),

$$\mu = -4\pi\gamma_o K_{oi},$$

and to the imaginary part of the ratio of the amplitude of the reflected to the incident wave through

$$\mu = \mu_o - 4\pi X_{oi}, \tag{5.1.5.1}$$

where X_{oi} is the imaginary part of X_o, which, using (5.1.2.24) and (5.1.3.10), is given by

$$X_o = R\lambda|C|\mathrm{S}(\gamma_h)(F_h F_{\bar{h}})^{1/2} \times \{\eta \pm [\eta^2 + \mathrm{S}(\gamma_h)]^{1/2}\}\big/\big[2\pi V(|\gamma|)^{1/2}\big]. \tag{5.1.5.2}$$

Taking the upper sign (+) for the $\pm$ term corresponds to tie points on branch 1 and taking the lower sign (−) corresponds to tie points on branch 2.

The calculation of the imaginary part X_{oi} is different in the Laue and in the Bragg cases. In the former case, the imaginary part of $(\eta^2 + 1)^{1/2}$ is small and can be approximated while in the latter, the imaginary part of $(\eta^2 - 1)^{1/2}$ is large when the real part of the deviation parameter, η_r, lies between 1 and −1, and cannot be calculated using the same approximation.

5.1.6. Intensities of plane waves in transmission geometry

5.1.6.1. Absorption coefficient

In transmission geometry, the imaginary part of X_o is small and, using a first-order approximation for the expansion of $(\eta^2 + 1)^{1/2}$, (5.1.5.1) and (5.1.5.2), the effective absorption coefficient in the absorption case is

$$\mu_j = \mu_o\left[\tfrac{1}{2}(1+\gamma^{-1}) \mp \frac{(\eta_r/2)(1-\gamma^{-1}) + |C|(\gamma^{-1})^{1/2}|F_{ih}/F_{io}|\cos\varphi}{(\eta_r^2+1)^{1/2}}\right], \tag{5.1.6.1}$$

where $\varphi = \varphi_{rh} - \varphi_{ih}$ is the phase difference between F_{rh} and F_{ih} [equation (5.1.2.10)], the upper sign (−) for the $\mp$ term corresponds to branch 1 and the lower sign (+) corresponds to branch 2 of the dispersion surface. In the symmetric Laue case ($\gamma = 1$, reflecting planes normal to the crystal surface), equation (5.1.6.1) reduces to

$$\mu_j = \mu_o\left[1 \mp \frac{|C||F_{ih}/F_{io}|\cos\varphi}{(\eta_r^2+1)^{1/2}}\right].$$

Fig. 5.1.6.1 shows the variations of the effective absorption coefficient μ_j with η_r for wavefields belonging to branches 1 and 2 in the case of the 400 reflection of GaAs with Cu $K\alpha$ radiation. It can be seen that for $\eta_r = 0$ the absorption coefficient for branch 1 becomes significantly smaller than the normal absorption coefficient, μ_o. The minimum absorption coefficient, $\mu_o(1 - |CF_{ih}/F_{io}|\cos\varphi)$, depends on the nature of the reflection through the structure factor and on the temperature through the Debye–Waller factor included in F_{ih} [equation (5.1.2.10*b*)] (Ohtsuki, 1964, 1965). For instance, in diamond-type structures, it is smaller for reflections with even indices than for reflections with odd indices. The influence of temperature is very important when $|F_{ih}/F_{io}|$ is close to one; for example, for germanium 220 and Mo $K\alpha$ radiation, the minimum absorption coefficient at 5 K is reduced to about 1% of its normal value, μ_o (Ludewig, 1969).

5.1.6.2. Boundary conditions for the amplitudes at the entrance surface – intensities of the reflected and refracted waves

Let us consider an infinite plane wave incident on a crystal plane surface of infinite lateral extension. As has been shown in Section 5.1.3, two wavefields are excited in the crystal, with tie points P_1 and P_2, and amplitudes D_{o1}, D_{h1} and D_{o2}, D_{h2}, respectively. Maxwell's boundary conditions (see Section A5.1.1.2 of the Appendix) imply continuity of the tangential component of the electric field and of the normal component of the electric displacement across the boundary. Because the index of refraction is so close to unity, one can assume to a very good approximation that there is continuity of the three components of both the electric field and the electric displacement. As a consequence, it can easily be shown that, *along the entrance surface*, for all components of the electric displacement

$$\begin{aligned} D_o^{(a)} &= D_{o1} + D_{o2} \\ 0 &= D_{h1} + D_{h2}, \end{aligned} \tag{5.1.6.2}$$

where $D_o^{(a)}$ is the amplitude of the incident wave.

Using (5.1.3.11), (5.1.5.2) and (5.1.6.2), it can be shown that the *intensities* of the four waves are

$$\begin{aligned} |D_{oj}|^2 &= |D_o^{(a)}|^2 \exp(-\mu_j z/\gamma_o)\big[(1+\eta_r^2)^{1/2} \mp \eta_r\big]^2 \times [4(1+\eta_r^2)]^{-1}, \\ |D_{hj}|^2 &= |D_o^{(a)}|^2 \exp(-\mu_j z/\gamma_o)|F_h/F_{\bar{h}}|[4\gamma(1+\eta_r^2)]^{-1}; \end{aligned} \tag{5.1.6.3}$$

top sign: $j = 1$; bottom sign: $j = 2$.